

Regulation of melanin-concentrating hormone receptor 1 signaling by RGS8 with the receptor third intracellular loop

Mayumi Miyamoto-Matsubara<sup>a</sup>, Osamu Saitoh<sup>b</sup>, Kei Maruyama<sup>c</sup>, Yoshimi Aizaki<sup>c</sup> and Yumiko Saito<sup>a,\*</sup>

<sup>a</sup>*Graduate School of Integrated Arts and Sciences, Hiroshima University, Kagamiyama, Hiroshima 739-8521, Japan;* <sup>b</sup>*Department of Bio-Science, Nagahama Institute of Bio-Science and Technology, Nagahama, Shiga 526-0829, Japan;* <sup>c</sup>*Department of Pharmacology, Saitama Medical School of Medicine, Iruma-gun, Saitama 350-0492, Japan*

Corresponding author. Tel.: +81-82-424-6563; fax: +81-82-424-0759

E-mail address: [yumist@hiroshima-u.ac.jp](mailto:yumist@hiroshima-u.ac.jp) (Y. Saito)

Abbreviations: CBB, Coomassie Brilliant Blue; DTT, dithiothreitol; ECL, enhanced chemiluminescence; FBS, fetal bovine serum; GAP, GTPase-activating protein; GPCR, G protein-coupled receptor; GST, glutathione S-transferase; HA, hemagglutinin; HEK293T, human embryonic kidney 293; His, histidine; i2 loop, second intracellular loop; i3 loop, third intracellular loop; IPTG, isopropyl- $\beta$ -D-thiogalactopyranoside; MCH, melanin-concentrating hormone; MCH1R, melanin-concentrating hormone receptor 1; MCH2R, melanin-concentrating hormone receptor 2; mAChR, muscarinic acetylcholine receptor; PTX, pertussis toxin; RGS, regulator of G protein signaling.

## **Abstract**

Melanin-concentrating hormone (MCH) receptor 1 (MCH1R) belongs to the class A G protein-coupled receptors (GPCRs). The MCH-MCH1R system plays a central role in energy metabolism, and thus the regulation of signaling pathways activated by this receptor is of particular interest. Regulator of G protein signaling (RGS) proteins work by increasing the GTPase activity of G protein  $\alpha$  subunits and attenuate cellular responses coupled with G proteins. Recent evidence has shown that RGS proteins are not simple G protein regulators but equally inhibit the signaling from various GPCRs. Here, we demonstrate that RGS8, which is highly expressed in the brain, functions as a negative modulator of MCH1R signaling. By using biochemical approaches, RGS8 was found to selectively and directly bind to the third intracellular (i3) loop of MCH1R in vitro. When expressed in HEK293T cells, RGS8 and MCH1R colocalized to the plasma membrane and RGS8 potently inhibited the calcium mobilization induced by MCH. The N-terminal 9 amino acids of RGS8 were required for the optimal capacity to downregulate the receptor signaling. Furthermore, Arg<sup>253</sup> and Arg<sup>256</sup> at the distal end of the i3 loop were found to comprise a structurally important site for the functional interaction with RGS8, since coexpression of RGS8 with R253Q/R256Q mutant receptors resulted a loss of induction of MCH-stimulated calcium mobilization. This functional association suggests that RGS8 may represent a new therapeutic target for the development of novel pharmaceutical agents.

**Key words:** MCH; MCH receptor; RGS protein; Calcium; Basic motif; Signaling complex

## Introduction

Distinct intracellular signaling pathways via activation of G protein-coupled receptors (GPCRs) are coupled to evoke distinct functional specificities in cells. Activation and inactivation of G proteins are highly regulated cellular events, and the regulator of G protein signaling (RGS) family of proteins are direct modulators of G protein activity. RGS proteins are extensively investigated as GTPase-activating proteins (GAPs) for heterotrimeric G protein  $G\alpha$  subunits. The proteins bind to the activated form of  $G\alpha$  and enhance its GTPase activity, thereby terminating  $G\alpha$ -dependent signaling [1]. Thus, RGS proteins reduce the maximal or steady-state levels of active G proteins and some RGS proteins also serve as effector antagonists to inhibit GPCR-mediated cellular signaling [1].

The members of the RGS protein family share a conserved RGS domain of approximately 120 amino acids, which is necessary and sufficient for binding to  $G\alpha$  and their GTPase-activating GAP activities [2]. Other than the RGS domain, the >30 family members are widely divergent. RGS proteins are classified into at least six subfamilies based on RGS domain identities, and related subfamily members also share conserved regions outside of their RGS domains [2,3]. Some RGS proteins, including members of the RA, R7 and R12 subfamilies, possess highly ordered structures with multiple functional domains. In contrast, the RZ and B/R4 subfamilies are simple, with relatively short featureless N- and C-terminal regions flanking the RGS domain. The RZ subfamily contains RGS17, 19 and 20, among which RGS19 was one of the first RGS proteins to be identified. The B/R4 subfamily contains the simplest RGS proteins. The members of this subfamily (RGS1, 2, 3, 4, 5, 8, 13 and 16) share a conserved amphipathic helix near their N-termini but have no other identifiable features outside of their RGS domains. These family members are often considered prototypical because they do not appear to have functions other than modulation of G protein activity.

By analyzing purified proteins *in vitro*, many RZ and B/R4 RGS proteins were found to nonselectively bind to and/or inhibit signaling by  $G\alpha_o$ ,  $G\alpha_i$ ,  $G\alpha_z$  and  $G\alpha_q$  [3]. However, subsequent studies revealed that some RGS proteins could function in living cells and selectively control the activities of specific G proteins. Furthermore, RGS proteins play roles beyond G protein regulation. It

has been reported that RGS proteins can distinguish GPCRs that are coupled to the same G protein when expressed in a whole-cell assay system [1-3]. RGS19 has been shown to preferentially regulate the  $G\alpha_i$ -coupled signaling of the ORL1 receptor over other opioid receptors [4]. RGS4 differentially inhibits signaling through  $G\alpha_q$ -coupled muscarinic acetylcholine or cholecystokinin receptors in cells [5]. Electrophysiological analyses in *Xenopus* oocytes revealed that RGS8 decreased the response upon activation of  $G\alpha_q$ -coupled M1 muscarinic acetylcholine receptor (mAChR) or substance P receptor, but did not remarkably inhibit the signaling from  $G\alpha_q$ -coupled M3 mAChR [6]. Furthermore, RGS1, 2, 4 and 16 displayed different relative potencies of their inhibitory activities toward signaling from  $G\alpha_q/11$ -linked muscarinic, bombesin or cholecystokinin receptors [7]. A separate study showed that RGS3, but not RGS1, 2 or 4, specifically inhibited gonadotropin-releasing hormone receptor-mediated inositol-1,4,5-triphosphate production in transfected COS cells [8]. Taken together, these results suggest that GPCRs possess intrinsic differential affinities for RGS proteins that determine their signaling functions. A recently discovered mechanism is that direct and selective interactions of RGS proteins with GPCRs are mediated through the receptor third intracellular (i3) loop [9-12] or the C-terminal domain [12]. Interestingly, the N-termini of RGS2, 4, 8 and 19, which do not contain the RGS domain, are necessary for receptor-type specific inhibition of signaling [4,5,9-12]. However, further understanding of the molecular mechanisms between GPCRs and RGS proteins requires much more information based on evaluation of the different receptor type-specific attenuations mediated by RGS proteins.

The orexigenic cyclic 19-amino-acid peptide melanin-concentrating hormone (MCH) [13] is the natural ligand for the class A GPCR MCH-1 receptor (MCH1R) [14,15]. The receptor is primarily expressed in the brain, where high expression of MCH1R mRNA is detected in the piriform cortex, olfactory tubercle, hippocampal formation, shell of the nucleus accumbens and amygdala [16]. A solid body of genetic and pharmacological evidence supports roles for MCH and MCH1R in the modulation of food intake and energy expenditure. Genetic ablation of both MCH [17] and MCH1R [18,19] in mice produces animals that are both lean and resistant to diet-induced obesity. Other studies have

indicated that acute and chronic administration of MCH enhances food intake and body weight [20] and that overexpression of MCH in transgenic mice leads to obesity and insulin resistance [21]. Although a second MCH receptor (MCH2R) has also been identified [22], its physiological role in these effects is unknown since genetic evidence indicates that mice do not express a functional form of this receptor [23]. High throughput screening efforts have led to the identification of small molecule MCH1R antagonists with diverse structural features and drug-like properties. In vivo results with these antagonists have indicated efficacy in several animal models of body weight regulation and feeding behavior [24]. Some of these antagonists also exhibit antidepressant and anxiolytic effects [25,26]. When expressed in heterologous cell lines, MCH1R is able to activate multiple signaling pathways, cyclic AMP inhibition, calcium mobilization and ERK through *Gai/o*- and *Gαq*-coupled pathways [14,15,27]. Mutagenesis and deletion studies of MCH1R have demonstrated that the second intracellular (i2) loop in the BBXXB motif (in which B is a basic residue and X is a nonbasic residue) and the proximal region of the C-terminal tail have profound functions for intracellular signaling pathways [28,29]. These observations suggest that there may be different determinants for modulating receptor-G protein activation. Recently, a yeast-two-hybrid approach identified MIZIP, periplakin and neurochondrin, which interact with the C-terminus of MCH1R [30-32]. Interaction of periplakin or neurochondrin with the proximal region of the C-terminus reduces the capacity of the receptor to initiate signaling. However, the mechanisms for how the GAP activity of MCH1R is modulated, and thus the mechanisms for how RGS proteins regulate MCH1R signaling, have not been examined and are largely unknown.

In the present study, we investigated whether there are direct physical interactions between RGS proteins and MCH1R that could dictate selectivity. In order to identify RGS proteins that interacted with MCH1R via its intracellular domains, we first focused on the i3 loop and generated GST fusion peptides of this domain to be used as affinity matrices for screening interacting RGS proteins in pull-down experiments. Our results demonstrated for the first time that (a) RGS8 in the B/R4 subfamily directly and selectively interacts with MCH1R via the i3 loop, (b) RGS8 suppresses

MCH1R-mediated calcium mobilization in human embryonic kidney 293 (HEK293) cells, and the N-terminus of RGS8 mediates the functional interaction with the MCH1R-i3 loop, and (c) both Arg<sup>253</sup> and Arg<sup>256</sup> in the BBXXB motif of the i3 loop are functionally influential for the interaction with RGS8. Our data provide the first example that a specific RGS protein interacts directly with MCH1R. Our results raise the possibility that RGS8 may have potential for therapeutic intervention in obesity.

## **2. Experimental procedures**

### *2.1. DNA construction*

The generation of a cDNA encoding a Flag epitope tag before the first methionine of rat MCH1R was described previously [28]. Flag-tagged rat MCH1R (Flag-MCH1R) was transfected into HEK293T cells to measure the receptor protein expression, surface expression and localization. Wild-type MCH1R and Flag-MCH1R have similar EC<sub>50</sub> values for MCH [28]. Rat M1 mAChR was a gift from Dr. T. Haga (Gakushuin University, Tokyo, Japan). MCH1R N-terminus, i2 loop, i3 loop and C-tail constructs were originally cloned into the PGEX-4T-1 vector to encode fusion proteins with an N-terminal GST tag. Each receptor fragment was amplified by PCR as a BamHI/XhoI fragment from the corresponding region of the rat full-length receptor as follows: N-terminus, amino acids 213-260; i2 loop, amino acids 233-280; i3 loop, amino acids 283-334; C-tail, amino acids 317-353. The fragments were isolated and subcloned in-frame with an N-terminal glutathione S-transferase (GST) tag into the pGEX4-1 vector. The open reading frames of all PCR-generated constructs were verified by nucleotide sequence analysis. Hemagglutinin (HA)<sub>3</sub>-tagged RGS2, 4, 8 and 19 were obtained from Missouri S&T cDNA Resource Center (Rolla, MO). RGS8 without an HA-tag was produced as described previously [6].

### *2.2. Induction and purification of GST fusion proteins*

GST-MCH1R fusion proteins (GST-MCH1R-N, GST-MCH1R-i2, GST-MCH1R-i3 and GST-MCH1R-C) were transformed into BL21(DE3) *Escherichia coli*. For each protein, 200-ml

cultures were grown in LB/carbenicillin and induced with 100  $\mu$ M isopropyl- $\beta$ -D-thiogalactopyranoside (IPTG) for 4 h at 25°C. Cells were centrifuged into a pellet, and soluble bacterial lysates were isolated using the B-PER bacterial protein expression reagent (Pierce, Rockford, IL) according to the manufacturer's protocol. The lysates were incubated with glutathione-Sepharose 4B beads (GE Healthcare UK Ltd., Little Chalfont, UK) for 1 h at 4°C with end-over-end rotation to allow binding of the fusion proteins. The resulting protein-bead complexes were washed three times with harvest buffer (10 mM Hepes pH 8.0, 50 mM NaCl, 5 mM EDTA, 1 mM dithiothreitol (DTT), 0.5% Triton X-100, Complete protease inhibitor, Mini, EDTA-free (Roche Diagnostics, Indianapolis, IN)), and then stored as a slurry in harvest buffer at -80°C. The concentrations of GST proteins bound to the glutathione resin varied among the GST fusion proteins. For each protein used, a single common batch of protein-bead complexes was generated and stored as aliquots at -80°C. The concentrations of bound proteins were determined by comparison of the Coomassie Brilliant Blue (CBB) staining intensities of the GST fusion proteins with known amounts of a protein standard (BSA). For experiments, the volume of beads used for each protein was adjusted to ensure that the same amount of total protein was used for binding interactions.

### *2.3. GST pull-down assays with HA-RGS proteins*

HEK293T cell lysates expressing HA-RGS proteins were mixed with GST or GST-MCH1R-i3 bound to glutathione-Sepharose beads (10-50  $\mu$ l) in harvest buffer with protease inhibitors. Equal amounts of GST fusion proteins (10  $\mu$ g) were added as determined by CBB staining. The total reaction volume was 250  $\mu$ l. Reactions were incubated by rotating overnight at 4°C. Beads were collected by centrifugation at 500 x g for 5 min at 4°C and sequentially washed four times with harvest buffer and once with harvest buffer without Triton X-100. Bound proteins were eluted from the beads by the addition of 2 x SDS sample buffer. The protein eluates were subjected to SDS-PAGE and electrotransferred to Hybond-P PVDF membranes (GE Healthcare UK Ltd.). The membranes were blocked with 5% skim milk in Tris-buffered saline containing 0.1% Tween 20 (TTBS) for 1 h,

incubated with an anti-HA antibody (3F10; Roche Diagnostics) for 2 h at room temperature, washed four times with TTBS and incubated with horseradish peroxidase-conjugated goat anti-rat IgG (GE Healthcare UK Ltd.) for 1 h. After four washes with TTBS, the reactive bands were visualized using an enhanced chemiluminescence (ECL) system (GE Healthcare UK Ltd.). After blotting, the membranes were stripped and reprobed with an anti-GST antibody (Nacalai Tesque, Kyoto, Japan).

#### *2.4. Expression and purification of recombinant RGS8 proteins*

Histidine (His)<sub>6</sub>-RGS8 and its variants were expressed and purified as previously described [11], with some modifications. The His-tagged protein constructs were introduced into *E. coli* M15[pREP4] (Qiagen, Hilden, Germany) and the bacteria were grown in Luria-Bertani broth containing ampicillin and kanamycin. The His-tagged proteins were induced with 1 mM IPTG for 4 h at 37°C. The cells were centrifuged into a pellet and suspended in sonication buffer (50 mM sodium phosphate pH 7.0, 1.3 M NaCl, 10% glycerol, 14 mM β-mercaptoethanol, 40 mM imidazole) supplemented with 1 mM PMSF. The fusion proteins were extracted by sonication and the samples were centrifuged. Ni<sup>2+</sup>-NTA agarose beads (Qiagen) were added to the cleared lysates and gently mixed on a rotator for 30 min at 4°C. After washing the complexes with sonication buffer, the fusion proteins were eluted with increasing concentrations of imidazole in a stepwise manner. The purified proteins were desalted and concentrated. The protein concentrations of the final solutions were estimated by the Bradford method and CBB staining following SDS-PAGE.

#### *2.5. GST pull-down assays with His-RGS8*

Assays for interactions between the GST-MCH1R-i3 loop and His-RGS8 proteins were performed as previously described [11]. Briefly, the GST-MCH1R-i3 fusion protein (2 μg) was mixed with the His-RGS8 protein (1 μg) in harvest buffer containing protease inhibitors and incubated overnight at 4°C on a rotator. After the overnight reaction, glutathione-Sepharose beads were added and incubated for 1 h at 4°C to recover the GST fusion proteins. Beads were collected by centrifugation and

sequentially washed three times with harvest buffer and once with harvest buffer without Triton X-100. Bound proteins were eluted from the beads by the addition of 2 x SDS sample buffer. Bound RGS proteins were detected by western blot analysis. After blotting with the anti-RGS8 antibody, the membranes were stripped and reprobed with an anti-GST antibody.

### *2.6. Mutagenesis of MCH1R*

Single-substitution mutations of the i3 loop were produced by oligonucleotide-mediated site-directed mutagenesis using a Quickchange site-directed mutagenesis kit (Stratagene, La Jolla, CA) [28,29]. All the mutations in the MCH1R cDNA sequence were confirmed by sequencing analysis. The mutated MCH1R cDNAs were excised by EcoRI and XhoI digestion and inserted into the pcDNA3.1 expression vector.

### *2.7. Cell culture and transfection*

HEK293T cells in 6-well plates were transiently transfected with Flag-MCH1R with or without vector or RGS proteins (total amount, 1.0 µg/well). DNA was mixed with the LipofectAMINE PLUS transfection reagent (Invitrogen, Carlsbad, CA), and the mixture was diluted with OptiMEM (Invitrogen) and added to HEK293T cells. The transfected cells were cultured in DMEM containing 10% fetal bovine serum (FBS). For calcium influx assays and immunocytochemistry, the cells were plated on 96-well plates and coverslips, respectively, at 24 h after transfection and cultured for a further 24 h.

### *2.8. Western blotting analyses for RGS proteins and Flag-MCH1R expressed in HEK293T cells*

To raise an antiserum against intact RGS8, rabbits were immunized with a keyhole limpet hemocyanin-conjugated synthetic peptide corresponding to residues 27-42 (N-terminal) of RGS8 using an immunization protocol as described previously [33]. The antibody obtained recognized an approximately 21-kDa polypeptide in RGS8-transfected HEK293T cells by western blotting (Fig. 2,

lower panel). No significant protein band was detected in mock vector-transfected HEK293T cells.

To generate whole-cell extracts, transiently transfected HEK293T cells were lysed with ice-cold SDS sample buffer (50 mM Tris-HCl pH 6.8, 2% SDS, 50 mM  $\beta$ -mercaptoethanol, 10% glycerol), and then homogenized by sonication at 4°C. For pull-down assays, we prepared detergent-soluble supernatants. Cells were lysed in ice-cold buffer (50 mM Tris-HCl pH 8.0, 150 mM NaCl, 1% Triton X-100, 0.1% SDS, 0.5% deoxycholate, Complete protease inhibitor mixture) at 4°C, and then cleared by centrifugation at 18,500 x *g* for 20 min at 4°C. For membrane preparations, cells were homogenized in ice-cold buffer (50 mM Tris-HCl pH 8.0, 150 mM NaCl, 10 mM MgCl<sub>2</sub>, 2 mM EDTA, Complete protease inhibitor mixture) using a glass/Teflon homogenizer and centrifuged at 800 x *g* for 10 min to remove the nuclei and cell debris. The resulting postnuclear supernatants were centrifuged at 100,000 x *g* for 1 h at 4°C. The resulting pellets were resuspended in ice-cold buffer (1% NP40, 50 mM Tris-HCl pH 8.0, 150 mM NaCl, 10 mM MgCl<sub>2</sub>, 2 mM EDTA, Complete protease inhibitor mixture) and incubated with rotation for 1 h at 4°C. The suspensions were further centrifuged at 100,000 x *g* for 1 h at 4°C, and the resulting supernatants were used as membrane preparations. The protein concentrations were determined using a BCA protein assay kit (Pierce). Aliquots of the total proteins were separated by SDS-PAGE and electrotransferred to PVDF membranes. After blocking, HA-RGS proteins and RGS8 on the membranes were detected using anti-HA and anti-RGS8 antibodies, respectively, followed by horseradish peroxidase-conjugated goat anti-rat or anti-rabbit IgG. The reactive bands were visualized with ECL substrates and analyzed using Scion Image (Scion Corporation, Frederick, MD). After blotting with the anti-RGS8 antibody, the membranes were stripped and reprobed with an anti-actin antibody (Chemicon, International Inc., Temecula, CA) or anti-Gαq/11 antibody (a gift from Dr. H. Ueda, Gifu University, Gifu, Japan).

### *2.9. Immunofluorescence microscopy*

Transiently transfected HEK293T cells were preincubated in Hanks-HEPES buffer (pH 7.5) for 1 h and then incubated with or without 1  $\mu$ M MCH for 1, 3, 5 or 15 min. Next, the cells were fixed,

permeabilized (0.05% Triton X-100 in PBS), blocked for 30 min and incubated with anti-Flag M2 and anti-RGS8 antibodies at 4°C overnight. The primary antibodies were detected using Alexa Fluor 488-conjugated goat anti-mouse IgG and Alexa Fluor 546-conjugated goat anti-rabbit IgG, respectively (both from Molecular Probes, Eugene, OR). Images were acquired using an FV1000 confocal microscope and imaging system (Olympus, Tokyo, Japan).

### *2.10. Measurement of intracellular $Ca^{2+}$*

Transiently transfected HEK293T cells seeded on 96-well plates (Becton Dickinson, Franklin Lakes, NJ) were loaded with a non-wash calcium dye (Calcium Assay Kit; Molecular Devices, Sunnyvale, CA) in Hank's balanced salt solution containing 20 mM HEPES (pH 7.5) for 1 h at 37°C. For each concentration of MCH or carbachol, the level of intracellular  $Ca^{2+}$  ( $[Ca^{2+}]_i$ ) was detected using a Flexstation II imaging plate reader (Molecular Devices) [28,29]. Data were expressed as the fluorescence (arbitrary units) versus time. The EC50 values for MCH or carbachol were obtained from sigmoidal fits using a nonlinear curve-fitting program (Prism version 3.0; GraphPad Software, San Diego, CA).

## **3. Results**

### ***3.1. The MCH1R-i3 loop selectively associates with RGS8***

MCH1R is highly expressed in the brain and responsible for feeding. Therefore, it seems to represent a promising target for anti-obesity treatments. Based on recent observations that RGS proteins can selectively inhibit signaling through different GPCRs [2,3], we hypothesized that some RGS proteins, which are highly expressed in the brain, interact selectively with MCH1R. To determine whether RGS proteins form stable complexes with MCH1R, we took advantage of an affinity binding pull-down assay that was previously used to identify binding partners for other GPCRs [9-11]. A fusion protein of GST with the i3 loop of MCH1R (GST-MCH1R-i3) or GST alone was expressed in bacteria and recovered by binding to glutathione-Sepharose beads. RGS proteins with N-terminal

3xHA tags (HA-RGS proteins) were transiently transfected into HEK293T cells. We selected RGS2, 4, 8 and 19 proteins for these experiments, since they are highly expressed in the brain [34-36]. Total cell lysates of these cells were incubated with equal protein amounts of the immobilized GST fusion protein or GST (Fig. 1A, Input). After collection and washing of the beads, the bound proteins were eluted by the addition of SDS sample buffer. Samples were subjected to SDS-PAGE and immunoblotting with an anti-HA antibody to detect bound HA-RGS proteins. We found that HA-RGS8 interacted with GST-MCH1R-i3 but not with GST alone (Fig. 1A, Pull-down). RGS2 was previously reported to bind to the i3 loop of M1 mAChR and i3 loop of  $\alpha$ 1A-adrenergic receptor [10], while RGS4 was found to bind to the i3 loop of M1 mAChR and i3 loop of receptor  $\delta$ -opioid receptor [12]. However, HA-RGS2, 4 and 19 did not interact with GST-MCH1R-i3. Next, we examined whether MCH1R-i3 contained a selective interactive region for RGS8. GST fusion proteins of the N-terminus, i2 loop and C-terminal tail were unable to bind HA-RGS8 (Fig. 1B). These results provide the first biochemical demonstration of a selective interaction between MCH1R and RGS8 through the i3 loop of MCH1R.

Our results indicated that RGS8 bound to the i3 loop of MCH1R in the HEK293T cell lysate, which contained native proteins involved in MCH1R signaling. Thus, the RGS8-MCH1R-i3 interaction in Fig. 1A may have resulted through other intermediate binding proteins in the cell lysate. To examine this possibility, we expressed N-terminally His-tagged recombinant RGS8 (His-RGS8) in bacteria and purified the protein using a nickel-nitrilotriacetic acid column (Fig. 1C). We found that purified His-RGS8 bound to GST-MCH1Ri3 in a similar manner to the protein in the cell lysate in Fig. 1A. Taken together, these results demonstrate that RGS8 binds directly and selectively to the i3 loop of MCH1R in the absence of other contributing factors.

### ***3.2. Coexpression of RGS8 with MCH1R at the cell membrane***

Next, we examined whether RGS8 associated with MCH1R at the same subcellular location when coexpressed in the same cell. When HEK293T cells were transfected with a plasmid encoding RGS8

alone, RGS8 was detected in the cytosol and plasma membrane by immunofluorescence microscopy (Fig. 2, RGS8 only upper panel). Localization in the nucleus was also observed in some cells. In contrast, untransfected HEK293T cells incubated with an anti-RGS8 antibody showed no significant immunostaining. When Flag-MCH1R and RGS8 were coexpressed, they were found together at the plasma membrane. Colocalization of Flag-MCH1R and RGS8 in the plasma membrane was also observed when Flag-MCH1R and HA-RGS8 were cotransfected and immunostained with anti-Flag M2 and anti-HA antibodies. Since coexpression of Flag-MCH1R did not seem to significantly promote RGS8 relocation to the plasma membrane from the cytosol (Fig. 2, upper panel), membrane-targeting factors intrinsic to RGS8 may exist [11] and this feature may be sufficient for its localization at the plasma membrane, as previously described for RGS2 and RGS4 [9,37]. We further assessed the cellular amounts of RGS8 by immunoblotting with an anti-RGS8 antibody (Fig. 2, lower panel). We compared the total amounts of RGS8 protein expressed in cells transfected with RGS8 with or without Flag-MCH1R. The intensities of the corresponding bands were quantified by imaging analysis, and the expression levels of the bands were found to be comparable (Fig. 2, left lower panel). Indeed, the intensity of the band in cells cotransfected with RGS8 and Flag-MCH1R was  $100.2 \pm 13.7\%$  (mean  $\pm$  SEM of four independent experiments) when the value in cells transfected with RGS8 alone was set as 100%. The amounts of RGS8 in the membrane fractions also remained unchanged in the presence or absence of Flag-MCH1R in three separate experiments ( $92.6 \pm 9.1\%$  in cells cotransfected with RGS8 and Flag-MCH1R vs. 100% in cells transfected with RGS8 alone) (Fig. 2, right lower panel). Thus, these results indicate that coexpression of Flag-MCH1R did not significantly affect the total cellular amounts of RGS8 or elicit translocation of RGS8 to the membrane fraction.

To examine the effects of receptor ligand binding and G protein activation, cells coexpressing MCH1R and RGS8 were stimulated with MCH. Addition of 1  $\mu$ M MCH for various times (1, 3, 5 or 15 min) did not alter the association of RGS8 with Flag-MCH1R at the plasma membrane (Fig. 2, upper panel). Immunoblotting analysis showed that treatment with MCH for 1 min did not cause translocation of RGS8 to the membrane fraction in three separate experiments ( $95.4 \pm 10.2\%$  in the

presence of MCH vs. 100% in the absence of MCH) (Fig. 2, right lower panel).

Taken together, these findings indicate that RGS8 and MCH1R are both present at the plasma membrane when coexpressed in the same cell, and that their formation is independent of downstream signaling events.

### ***3.3. RGS8 inhibits MCH1R-mediated calcium signaling***

To assess the functional effects of RGS8 on cellular responses mediated by G proteins, we compared calcium mobilization mediated by MCH1R expressed with or without recombinant RGS8 in HEK293T cells. Representative curves are shown in Fig. 3. Coexpression of RGS8 significantly blocked calcium signaling by MCH. Next, to determine whether a certain concentration of cellular RGS8 is required to inhibit G protein-dependent signaling, we transfected cells with graded amounts of the RGS8 plasmid (Fig. 3), leading to the production of graded cellular amounts of RGS8 protein. Table 1 shows the EC<sub>50</sub> values of MCH for Flag-MCH1R and RGS8. Cells transfected with 0.8 µg of RGS8 and 0.2 µg of Flag-MCH1R exhibited a 19-fold higher EC<sub>50</sub> value and a 20% reduction in the maximal response. Even cells cotransfected with 0.2 µg of RGS8 showed significant inhibition of MCH1R-mediated calcium signaling with a 7-fold higher EC<sub>50</sub> value (Table 1).

MCH1R couples with multiple G proteins and activates diverse signal transduction pathways that include both cAMP inhibition and calcium influx facilitation [14,15,27], while MCH2R exclusively couples with G $\alpha$ q [22]. GPCRs are known to stimulate the activation of phospholipase C $\beta$  (PLC $\beta$ ) isoforms via either G $\alpha$ q or G $\beta$ v dimers released from activated G $\alpha$ o/i, whereas only G $\alpha$ o/i-mediated PLC $\beta$  activation is inhibited by pertussis toxin (PTX), which specifically blocks signaling by receptors that activate Go/i proteins. To confirm which G $\alpha$  protein is involved in the stimulation of PLC $\beta$  by Flag-MCH1R, we pretreated transfected cells with PTX. After cells transfected with Flag-MCH1R (0.2 µg) were pretreated with 200 ng/ml PTX for 20 h, the effect of MCH on the calcium influx was partially inhibited, but not abolished (decrease of -20% compared with the maximal response), consistent with previous reports [28,29]. The EC<sub>50</sub> value in PTX-treated cells was 9.0 ± 0.9 nM,

whereas that in untreated cells was  $2.1 \pm 0.3$  nM (mean  $\pm$  SEM of three independent experiments), and the +PTX ( $G\alpha_q$ -dependent response)/-PTX ( $G\alpha_o/i$ -independent response) ratio was 4.30. These results indicate that both PTX-sensitive  $G\alpha_i/o$  and PTX-insensitive  $G\alpha_q$  mediate the mobilization of intracellular calcium in response to MCH, and that a large component of the calcium influx is dependent on  $G\alpha_q$  activity rather than  $G\alpha_i/o$  activity.

RGS8 was found to preferentially bind  $G\alpha_o$  and  $G\alpha_i3$  using in vitro binding assays [34]. Despite its weak binding to  $G\alpha_q$  protein, RGS8 showed  $G\alpha_q$ -coupled responses in a cellular environment. Use of the *Xenopus* oocyte system to investigate the regulatory effects of RGS8 on the  $G\alpha_q$ -coupled responses revealed that RGS8 decreased the responses upon activation of M1 mAChR or substance P receptor [6]. Therefore, we next examined whether the effectiveness of RGS8 in blocking calcium signaling was mediated by  $G\alpha_q$  and/or  $G\alpha_o/i$  in Flag-MCH1R-expressing cells. When cells transfected with 0.8  $\mu$ g of RGS8 and 0.2  $\mu$ g of Flag-MCH1R were pretreated with PTX, the EC50 value was  $56.7 \pm 4.7$  nM. Since the EC50 value in PTX-treated cells transfected with Flag-MCH1R alone was  $9.0 \pm 0.9$  nM, RGS8 inhibited MCH1R-mediated calcium signaling with a 6.3-fold higher EC50 value under conditions that blocked  $G\alpha_o/i$ -mediated signaling. On the other hand, cells cotransfected with RGS8 and Flag-MCH1R without PTX treatment had a 19-fold higher EC50 value (Table 1). If RGS8 only attenuated  $G\alpha_q$ -mediated calcium signaling, the extent of inhibition should be nearly identical regardless of PTX treatment. Collectively, these results suggest that RGS8 inhibits MCH1R signaling by inhibiting the actions of both  $G\alpha_q$  and  $G\alpha_o/i$ .

### ***3.4. Evidence for an interaction between the N-terminus of RGS8 and MCH1R***

It has been shown that the N-terminal domains of RGS proteins are required to promote their associations with  $G\alpha$  subunits and GPCRs [4,5,9-11]. Therefore, we examined the capacity of the N-terminal portion of RGS8 to inhibit the signaling of Flag-MCH1R (Fig. 4). RGS8S is a short isoform of RGS8, which arises due to alternative splicing of the RGS8 gene. The RGS8S cDNA encodes 7 unique N-terminal amino acids instead of the normal amino acids 1-9 of RGS8 (6), while

the rest of RGS8S is the same as RGS8 (Fig. 4A). We transiently transfected cells with Flag-MCH1R with or without RGS8S constructs, and also performed western blot analyses with an anti-RGS8 antibody to compare the amounts of RGS8S protein expression. Although similar amounts of the exogenous RGS proteins were expressed in the cells, RGS8S exhibited a 2.2-fold lower efficacy than RGS8 (Fig. 4B, Table 1). Since RGS8 and RGS8S only differ by 9 N-terminal amino acids, we tested the relative capacities of RGS8 and a truncated form of RGS8,  $\Delta$ N9, which lacked the first 9 N-terminal amino acids. When the expression levels were identical,  $\Delta$ N9 showed a similar reduction in activity to RGS8S (Table 1). In separate assays, we compared the capacities of authentic RGS8 and  $\Delta$ N9 to bind GST-MCH1R-i3 protein. The level of binding of  $\Delta$ N9 to GST-MCH1R-i3 was decreased by 33% (Fig. 4C). Taken together, these data suggest that the N-terminal 9 amino acids of RGS8 are necessary for optimal inhibition of MCH1R function.

As described above, a previous study showed that RGS8 blocks M1 mAChR-mediated regulatory function in *Xenopus* oocytes, as evaluated by an increase in  $\text{Ca}^{2+}$ -activated  $\text{Cl}^-$  currents [6]. The assay system demonstrated the importance of the N-terminal 9 amino acids of RGS8 for M1 mAChR-specific suppression [11]. By using the HEK293T system, we tested the extents of inhibition of RGS8, RGS8S and  $\Delta$ N9 on M1 mAChR-mediated functions stimulated by carbachol (Table 1). Coexpression of RGS8 caused inhibition of M1 mAChR-induced calcium mobilization with a 15-fold higher  $\text{EC}_{50}$  value without significantly changing the maximum response, while RGS8S and  $\Delta$ N9 only showed 2.8- and 2.6-fold higher  $\text{EC}_{50}$  values, respectively. Thus, deletion of the N-terminal 9 amino acids of RGS8 caused a more dramatic reduction in the potency of M1 mAChR-mediated signaling (5.6-fold lower) compared to that of Flag-MCH1R (2.2-fold lower). These results suggest that the requirement of the N-terminal 9 amino acids of RGS8 for receptor signaling is not identical between M1 mAChR and Flag-MCH1R.

To further understand the mechanism behind MCH1R inhibition by RGS8, we examined the roles of the RGS domain. A point mutation in the RGS domain of RGS8 (L153F) has been shown to greatly reduce the affinity for  $\text{G}\alpha$  and cause defective inhibition of G-protein signaling [38]. Therefore, we

investigated how the L153F mutant affected  $G\alpha_q$  signaling from Flag-MCH1R (Fig. 4B). It was clearly found that the inhibition of  $G\alpha_q$  signaling by L153F was quite weak, in comparison with the suppressive activity of RGS8. These data indicate that RGS8 is unable to suppress  $G\alpha$ -coupled signaling effectively without the intact GAP function of the RGS domain. Therefore, it is considered that both the N-terminal 9 amino acids and the RGS domain of RGS8 are necessary for the optimal capacity to attenuate Flag-MCH1R-mediated signaling.

### ***3.5. The distal region of the MCH1R-i3 loop comprises a structurally important site for the interaction with RGS8***

Since RGS8 directly associates with the i3 loop of Flag-MCH1R, we wondered which amino acid residues within the i3 loop were involved in altering this functional interaction. Saitoh et al. [11] reported that the C-terminus of the M1 mAChR-i3 loop is the specific site for RGS8 association. We previously created a variety of MCH1R mutants including a structural BBXXB motif. Therefore, we took advantage of our experience to select six substitution mutants in which the basic residues at the C-terminus of the i3 loop were replaced with neutrally charged glutamine residues. The levels of receptor expression of single-substitution (R248Q, K252Q, R253Q and R256Q), R253Q/R256Q and K252Q/R253Q/R256Q mutants were identical to that of Flag-MCH1R [29,39] (Fig. 5A). Previous radioligand binding experiments using cell membrane preparations revealed that the maximal binding capacity ( $B_{max}$ ) values of the single-substitution, R253Q/R256Q and K252Q/R253Q/R256Q mutants were similar to that of Flag-MCH1R, while the values of affinity constants ( $K_d$ ) for the R253Q/R256Q and K252Q/R253Q/R256Q mutants were decreased by 2- and 3-fold, respectively [29]. Regarding stimulation of a calcium influx, R248Q and K252Q had almost no effect [30,39], whereas both R253Q and R256Q caused approximately 4-fold increases in the  $EC_{50}$  values (Table 2) [29]. For R253Q/R256Q and K252Q/R253Q/R256Q, the apparent  $EC_{50}$  values of MCH were increased by 28- and 50-fold, respectively, while these mutant receptors showed similar maximal responses to MCH1R (Table 2, Fig. 5A) [29].

Each receptor mutant was transiently transfected into cells alone or in combination with RGS8 and assayed for MCH-stimulated calcium mobilization. The levels of receptor expression and RGS8 expression were determined by immunoblotting analyses of the transfected cells using anti-Flag M2 and anti-RGS8 antibodies, respectively (Fig. 5A). Coexpression of RGS8 did not significantly affect the amounts of R253Q/R256Q and K252Q/R253Q/R256Q. Similarly, the amounts of RGS8 were equivalent between R253Q/R256Q- and K252Q/R253Q/R256Q-expressing cells.

As shown in Table 2 and Fig. 5B, RGS8 only caused a loss of function for stimulating calcium mobilization in K252Q/R253Q/R256Q- and R253Q/R256Q-expressing cells. Since the inhibitory effects of RGS8 in cells expressing the single-substitution mutants (R248Q, K252Q, R253Q and R256Q) were identical to that of cells expressing Flag-MCH1R (Table 2), simultaneous mutations of Arg<sup>253</sup> and Arg<sup>256</sup> in the BBXXB motif, at least, are necessary to produce a drastic increase in RGS8 inhibition of the receptor functional responses. Next, we examined whether the functional enhancement of RGS8 with the R253Q/R256Q mutant was correlated with an increase in the binding between them. For this purpose, the MCH1R mutant construct was expressed as a GST fusion protein containing the R253Q/R256Q mutations. Purified His-RGS8 protein was incubated with the GST fusion protein and subjected to a pull-down assay. His-RGS8 protein bound the GST fusion protein containing the R253Q/R256Q mutations with a similar affinity to its affinity for the GST fusion protein containing the non-mutated i3 loop (Fig. 5C). Thus, the increase in RGS8 inhibition of the R253Q/R256Q receptor functional responses was not simply caused by an increase in binding between RGS8 and the GST-i3-R253Q/R256Q loop. These results show that Arg<sup>253</sup> and Arg<sup>256</sup> in the basic motif of the i3 loop comprise a structurally important site for functional interaction with RGS8 in the context of a cellular environment.

#### **4. Discussion**

In the present study, we have identified RGS8 as a negative modulator of MCH1R-mediated signaling. First, we found that RGS8 selectively and directly interacted with MCH1R via the receptor

i3 loop. This interaction also occurred in living cells. MCH1R-mediated calcium mobilization was markedly attenuated by RGS8 through  $G\alpha_q$  and  $G\alpha_o/i$ -mediated pathways in HEK293T cells. The inhibition by RGS8 was dose-dependent, since higher expression levels of RGS8 further reduced the efficacy to induce calcium mobilization. Next, we examined which region is functionally important for the RGS8-MCH1R interaction, and found that both the N-terminal 9 amino acids and the RGS domain of RGS8 were involved in effective attenuation of the signaling evoked by MCH1R. Further analyses with site-directed mutagenesis of the i3 loop of MCH1R were performed in combination with RGS8. This approach revealed that simultaneous mutations of Arg<sup>253</sup> and Arg<sup>256</sup> located at the C-terminus of the i3 loop increased RGS8 antagonist activity. To date, only the proximal C-terminus of MCH1R has been identified as being involved in binding to other functional molecules [31,32]. Therefore, our present data provide the first evidence that the proximal region of the i3 loop in addition to the C-terminus is a protein-binding site that changes the receptor function.

There is growing evidence from a variety of functional assay systems that the N-terminal domains of RGS proteins are involved in GPCR-selective inhibition, whereas the conserved RGS domains act as GAPs [4,5,9-11,40]. It therefore seemed likely that the affinities of the N-terminal domains of RGS proteins for particular GPCRs are critical for controlling the specificity and high-potency inhibition of receptor-coupled signaling in intact cells [3,9]. However, a few reports have addressed the possibility of direct interactions of the N-terminal domains of RGS proteins with GPCRs in cellular environments [5,9-11,40]. B/R4 RGS proteins have been proposed to contain an N-terminal amphipathic helix that seems to be important for proper plasma membrane association [1,2]. In the case of RGS2, the first 78 N-terminal amino acids are required for its association with M1 mAChR and  $\alpha 1A$ -adrenergic receptor and inhibition of their signaling [9,10]. A recent study showed that RGS2 contains unique hydrophobic residues adjacent to the core amphipathic helix domain that are responsible for increased functions toward M1 mAChR [40]. RGS8 also blocks M1 mAChR-mediated regulatory functions in *Xenopus* oocytes by increasing  $Ca^{2+}$ -activated  $Cl^-$  currents [6]. It has been shown that deletion of the N-terminal 9 amino acids of RGS8 ( $\Delta N9$ ) dramatically decreases the binding affinity for the M1 mAChR-i3 loop

and thus reduces its capacity to inhibit M1 mAChR-mediated signaling in *Xenopus* oocytes [11]. The functional importance of the N-terminal 9 amino acids of RGS8 was confirmed in our mammalian system, in which M1 mAChR-mediated signaling was monitored by calcium mobilization in receptor-transfected HEK293T cells. On the other hand, we found that the same 9 amino acids of RGS8 were also important for association with MCH1R and modulation of its signaling. However,  $\Delta$ N9 had a more severe effect on M1 mAChR signaling (5.6-fold decrease) than on Flag-MCH1R signaling (2.2-fold decrease). These findings are roughly consistent with the results of in vitro pull-down assays with GST fusion proteins, since the binding of His- $\Delta$ N9 to M1 mAChR-i3 was drastically reduced by more than 80% compared with full-length RGS8 [11], while the binding of His- $\Delta$ N9 to MCH1R-i3 was reduced by 33%. These results indicate that the contact site in RGS8 for the MCH1R-i3 loop includes the N-terminal 9 amino acids, although the affinities of these amino acids differ for the MCH1R-i3 and M1 mAChR-i3 loops. It remains unclear which sites in RGS8 produce the key regulatory specificities toward MCH1R. By predicting secondary models and creating chimeras with other RGS proteins [38,40], the regions of RGS8 that are selective and sufficient for binding to MCH1R and for displaying RGS8 antagonist activity toward MCH1R will be clarified.

Unlike characterization of the receptor-binding sites within RGS proteins, only a few studies have addressed the issue of which regions in GPCRs are involved in associations with RGS proteins. It has been shown that the RGS-binding sites within GPCRs are located in the i3 loop [9-12] and/or the C-terminus [12]. Both RGS2 and RGS4 have been reported to bind to the M1 mAChR-i3 loop, but their binding sites within the i3 loop have not been characterized. On the other hand, it has been shown that RGS8 can interact with the C-terminus of the M1 mAChR-i3 loop [11]. Moreover, the RGS2-binding site was found to be located in the N-terminal proximal half (Lys<sup>219</sup>, Ser<sup>220</sup> and Ser<sup>238</sup>) of the  $\alpha$ 1A-adrenergic receptor-i3 loop, since mutations of these residues led to a loss of binding with the receptor and resulted in decreased RGS2-mediated inhibition of receptor functional responses [10]. In contrast, our mutations in the BBXXB motif at the C-terminus of the MCH1R-i3 loop accelerated RGS8 antagonist activity, and caused a loss of calcium mobilization by MCH.

A number of mutagenesis approaches have implied that the i3 loop is an important signaling structure in the GPCR superfamily. In particular, a BBXXB motif at the end of the i3 loop and into the N-terminus of transmembrane domain 6 has been shown to regulate GPCR activities, since mutations in this region can disrupt receptor coupling to G proteins or lead to constitutive activation of the receptors [41,42]. We previously examined the functional role of the BBXXB motif in the i3 loop of MCH1R [28]. We found that the K252Q/R253Q/R256Q and R253Q/R256Q mutants in the motif still activated calcium mobilization with changes in the high affinity constant, but retained identical maximal responses to that of Flag-MCH1R. Thus, the basic motif in the i3 loop of MCH1R seems to function in the packing of the transmembrane domains of MCH1R, resulting in either decreased accessibility of the G protein coupling site or inability of the receptor to form an active conformation upon MCH binding. Simultaneous mutations of Arg<sup>253</sup> and Arg<sup>256</sup> in the motif, at least, produced a drastic increase in RGS8-mediated inhibition of the receptor function, and the present data therefore provide new information regarding the role of the i3 loop in MCH1R. Thus, the basic motif in the i3 loop also comprises a structurally important region for interacting with RGS8 and modulating the signaling pathway in living cells.

Even though we have indicated the importance of Arg<sup>253</sup> and Arg<sup>256</sup> for functional interaction with RGS8, it remains unclear how the R253Q/R256Q receptor enhanced RGS8 antagonist activity. We can speculate that the conformational change caused by R253Q/R256Q may help to localize and orient RGS8 to increase the GAP activity towards G proteins. It may also be possible that the conformational change induced by R253Q/R256Q allows RGS8 to couple with other cytoplasmic intracellular loops and/or additional unidentified accessory proteins including G proteins, thereby resulting in enhanced GAP activity. Alternatively, the three-dimensional structure induced by the interaction between R253Q/R256Q and RGS8 may contribute to a loss of function of receptor activity. In any case, it is likely that an appropriate physical complex between RGS8 and the C-terminal basic motif of the i3 loop in MCH1R is responsible for integrating the signaling efficiency. Further studies on systematic combinations of RGS8 with different MCH1R mutants are required to clarify the molecular dynamics

controlling the recognition between RGS8 and MCH1R.

In summary, the present study has demonstrated that RGS8 is a negative modulator of MCH1R-mediated calcium signaling. MCH1R is a well validated target for potential therapeutic intervention in obesity. It is highly expressed in the brain, including the olfactory tubercle, hippocampal formation, nucleus accumbens and amygdala [16]. On the other hand, RGS8 is highly expressed in brain areas such as the cerebellum, olfactory tubercle, hippocampal formation and nucleus accumbens [34,35]. Finding evidence for MCH signaling modulation by RGS8 in the olfactory tubercle, hippocampal formation and nucleus accumbens is of particular interest, since these regions are important in olfaction/feeding and motivated behavior/feeding. Studies of RGS proteins have provided insights into disease pathways, such as the contributions of RGS2 to hypertension and RGS4/RGS9-2 to drug addiction [3,43]. Similarly, regulation by RGS8 may represent a new avenue for research into the mechanisms of MCH1R regulation in the nervous system and may lead to the development of novel drugs for treating disorders where modulation of MCH1R activity has therapeutic potential.

### **Acknowledgements**

This study was supported by research grants from the Ministry of Education, Science, Sports and Culture of Japan (to YS and OS) and from the Takeda Science Foundation (to OS). The authors would like to thank Akiko Kojo for technical assistance.

## References

- [1] S. Hollinger, J.R. Hepler, *Pharmacol. Rev.* 54 (2002) 527.
- [2] E.M. Ross, T.M. Wilkie, *Annu. Rev. Biochem.* 69 (2000) 795.
- [3] G.B. Willars, *Sem. Cell Dev. Biol.* 17 (2006) 364.
- [4] G-X. Xie J, Y. Yanagisawa, E. Ito, K. Maruyama, X. Hang, K.J. Kim, K.R. Han, K. Moriyama, P.P. Palmer, *J. Mol. Biol.* 353 (2005) 1081.
- [5] W. Zeng, X. Xu, S. Popov, D.M. Berman, I. Davignon, K. Yu, D. Yowe, S. Offermanns, S. Muallem, T.M. Wilkie, *J. Biol. Chem.* 273 (1998) 34687.
- [6] O. Saitoh, Y. Murata, M. Odagiri, M. Itoh, H. Itoh, T. Misaka, Y. Kubo Y, *Proc. Natl Acad. Sci. USA* 99 (2002)10138.
- [7] X, Xu, W, Zeng, S. Popov, D, M. Berman, I, Davignon, D. Yowe, S. Offermanns, S. Muallem, T.M. Wilkie T, *J. Biol. Chem.* 274 (1999) 3549.
- [8] J.D. Neill, L.W. Duck, J.C. Sellers, L.C.Musgrove, A. Scheschonka, K.M. Druey, J.H. Kehrl, *Endocrinology* 138 (1997) 843.
- [9] L.S. Bernstein, S. Ramineni, C. Hague, W. Cladman, P. Chidiac, A.I. Levey, J.R. Hepler, *J. Biol. Chem.* 279 (2004) 21248.
- [10] C. Hague, L.S. Bernstein, S. Ramineni, Z, Chen, K.P. Minneman, J.R. Hepler, *J. Biol. Chem.* 280 (2005) 27289.
- [11] M. Itoh, K. Nagatomo, Y. Kubo, O. Saitoh, *J. Neurochem.* 99 (2006) 1505.
- [12] Z. Georgoussi, L. Leontiadis L, G. Mazarakou, M. Merkouris, K. Hyde, H. Hamm, *Cell Signal.* 18 (2006) 771.
- [13] H. Kawauchi, I. Kawazoe, M. Tsubokawa, M. Kishida, B.I. Baker, *Nature* 305 (1983) 321.
- [14] J. Chambers, R.S. Ames, D. Bergsma, A. Muir, L.R. Fitzgerald, G. Hervieu, G.M. Dytko, J.J. Foley, J. Martin, W.S. Liu, J. Park, C. Ellis, S. Ganguly, S. Konchar, J. Cluderray, R. Leslie, S. Wilson, H.M. Sarau, *Nature* 400 (1999) 261.
- [15] Y. Saito, H.P. Nothacker, Z. Wang, S.H.S. Lin, F. Leslie, O. Civelli, *Nature* 400 (1999) 265.

- [16] Y. Saito, M. Cheng, F.M. Leslie, O. Civelli, J. Comp. Neurol 435 (2001) 26.
- [17] M. Shimada, N.A. Tritos, B.B. Lowell, J.S. Flier, E. Maratos-Flier, Nature 396 (1998) 670.
- [18] D.J. Marsh, D.T. Weingarh, D.E. Novi, H.Y. Chen, M.E. Trumbauer, A.S. Chen, X.M. Guan, M.M. Jiang, Y. Feng, R.E. Camacho, Z. Shen, E.G. Frazier, H. Yu, J.M. Metzger, S.J. Kuca, L.P. Shearman, S. Gopal-Truter, D.J. MacNeil, A.M. Strack, D.E. MacIntyre, L.H. Van der Ploeg, S. Qian, Proc. Natl. Acad. Sci. U.S.A. 99 (2002) 3240.
- [19] Y. Chen, C. Hu, C.K. Hsu, Q. Zhang, C. Bi, M. Asnicar, H.M. Hsiung, N. Fox, L.J. Sliker, D.D. Yang, M.L. Heiman, Y. Shi, Endocrinology 143 (2002) 2469.
- [20] D. Qu, D.S. Ludwig, S. Gammeltoft, M. Piper, M.A. Peleymounter, M.J. Cullen, W.F. Mathes, J. Przypek, R. Kanarek, E. Maratos-Flier, Nature 380 (1996) 243.
- [21] D.S. Ludwig, K.G. Mountjoy, J.B. Tatro, J.A. Gillette, R.C. Frederich, J.S. Flier, E. Maratos-Flier, Am. J. Physiol 274 (1998) E627.
- [22] J. Hill, M. Duckworth, P. Murdock, G. Rennie, C. Sabido-David, R.S. Ames, P. Szekeres, S. Wilson, D.J. Bergsma, I.S. Gloger, D.S. Levy, J.K. Chambers, A.I. Muir, J. Biol. Chem. 276 (2001) 20125.
- [23] C.P. Tan, H. Sano, H. Iwaasa, J. Pan, A.W. Sailer, D.L. Hreniuk, S.D. Feighner, O.C. Palyha, S.S. Pong, D.J. Figueroa, C.P. Austin, M.M. Jiang, H. Yu, J. Ito, M. Ito, X.M. Guan, D.J. MacNeil, A. Kanatani, L.H. Van der Ploeg, A.D. Howard, Genomics 79 (2002) 785.
- [24] S. Takekawa, A. Asami, Y. Ishihara, J. Terauchi, K. Kato, Y. Shimomura, M. Mori, H. Murakoshi, K. Kato, N. Suzuki, O. Nishimura, M. Fujino, Eur. J. Pharmacol. 438 (2002) 129.
- [25] B. Borowsky, M.M. Durkin, K. Ogozalek, M.R. Marzabadi, J. DeLeon, B. Lagu, R. Heurich, H. Lichtblau, Z. Shaposhnik, I. Daniewska, T.P. Blackburn, T.A. Branchek, C. Gerald, P.J. Vaysse, C. Forray, Nat. Med. 8 (2002) 825.
- [26] S. Chaki, T. Funakoshi, S. Hirota-Okuno, M. Nishiguchi, T. Shimazaki, M. Iijima, A.J. Grottick, K. Kanuma, K. Omodera, Y. Sekiguchi, S. Okuyama, T.A. Tran, G. Semple, W. Thomsen, J. Pharmacol. Exp. Ther. 313 (2005) 831.

- [27] B.E. Hawes, E. Kil, B. Green, K. O'Neill, S. Fried, M.P. Graziano, *Endocrinology* 141 (2000) 4524.
- [28] M. Tetsuka, Y. Saito, K. Imai, H. Doi, K. Maruyama, *Endocrinology* 145 (2004) 3712.
- [29] Y. Saito, M. Tetsuka, S. Saito, K. Imai, A. Yoshikawa, H. Doi, K. Maruyama, *Endocrinology* 146 (2005) 3452.
- [30] D. Bachner, H. Kreienkamp, D. Richter, *FEBS Lett* 526 (2002) 124.
- [31] H. Murdoch, G.-J. Feng, D. Bachner, L. Ormiston, J. H. White, D. Richter, G. Milligan, *J. Biol. Chem.* 280 (2005) 8208.
- [32] F. Francke, R. J. Ward, L. Jenkins, E. Kellett, D. Richter, G. Milligan, D. Bachner, *J. Biol. Chem.* 281 (2006) 32496.
- [33] M. Itoh, M. Odagiri, H. Abe, O. Saitoh, *Biochem. Biophys. Res. Commun.* 287 (2001) 223.
- [34] O. Saitoh, Y. Kubo, Y. Miyatani, T. Asano, H. Nakata H, *Nature* 390 (1997) 525.
- [35] E. Grafstein-Dunn, K. H. Young, M. I. Cockett, X.Z. Khawaja, *Mol. Brain. Res.* (2001) 113.
- [36] S. J. Gold, Y.G. Ni, H. G. Dohlman, E. J. Nestler, *J. Neurosci.* (1997) 8037.
- [37] L.S. Bernstein, A.A. Grillo, S.S. Loranger, M.E. Linder, *J. Biol. Chem.* 275 (2000) 18520.
- [38] I. Masuho, M. Itoh, H. Itoh, O. Saitoh, *J. Neurochem.* 88 (2004) 161.
- [39] W.T. Gibson, P. Pissios, D.J. Trombly, J. Luan, J. Keogh, N.J. Wareham, E. Maratos-Flier, S. O'Rahilly, I.S. Farooqi, *Obesity Research* 12 (2004) 743.
- [40] S. Gu, W-T. Ho, S. Ramineni, D.M. Thal, R. Natesh, J.J.G. Tesmer, J.R. Hepler, S.P. Heximer, *J. Biol. Chem.* 282 (2007) 33064.
- [41] D. Wu, H. Jiang, M.I. Simon, *J. Biol. Chem.* 270 (1995) 9828.
- [42] P.J. Pauwels, A. Gouble, T. Wurch, *Biochem. J.* 343 (1999) 435.
- [43] S.B. Hooks, K. Martemyanov, V. Zachariou, *Biochem. Pharmacol.* 75, (2008) 76.

## Figure legends

### **Fig. 1. Interaction between RGS8 and the MCH1R-i3 loop.**

**A,** The MCH1R-i3 loop selectively interacts with 3xHA-RGS8 in cell lysates. Cell lysates from HEK293T cells transfected with 3xHA-RGS2, 4, 8 or 19 were incubated with equal amounts of GST-MCH1R-i3 or GST alone (10  $\mu$ g) and bound to glutathione-Sepharose beads. The beads were harvested, washed by centrifugation and suspended in SDS sample buffer to elute the bound proteins. Aliquots (20%) of the protein eluates were separated by SDS-PAGE using a 15% gel, transferred to PVDF membranes and subjected to western blot analysis using an anti-HA antibody to detect bound RGS proteins (Pull-down, IB:HA). The amounts of GST fusion proteins loaded were verified by reprobing with an anti-GST antibody (IB:GST; Nacalai Tesque, 1:4000). Blots were developed with an ECL kit. The results are representative of at least three independent experiments. (Input) The cell lysate loaded in each lane represents the total amount of HA-RGS protein in the cell lysate used for each reaction. The amount of each GST fusion protein was adjusted to 0.2  $\mu$ g. **B,** Interactions between the N-terminus, i2 loop, i3 loop and C-terminal tail of MCH1R and 3xHA-RGS8. GST alone or GST fusion proteins incorporating the predicted N-terminus, i2 loop, i3 loop and C-terminal tail of MCH1R were expressed and used in pull-down assays that included HA-RGS8 as described for (A). Aliquots (20%) of the protein eluates were separated by SDS-PAGE using a 15% gel and subjected to western blot analysis using an anti-HA antibody to detect bound RGS proteins (Pull down, IB:HA). The amounts of GST fusion proteins loaded were verified by reprobing with an anti-GST antibody. The experiments were repeated three times. (Input) The cell lysate loaded in the lane represents the total amount of HA-RGS8 proteins in the cell lysate used for each reaction. The amount of each MCH1R subdomain-GST fusion protein was adjusted to 0.2  $\mu$ g. **C,** RGS8 binds directly to the MCH1R-i3 loop. 6xHis-RGS8 was expressed in *E. coli* and purified by nickel-nitrilotriacetic acid affinity chromatography. Purified His-RGS8 (1  $\mu$ g) was incubated with 2  $\mu$ g of GST-MCH1R-i3 or GST alone and bound to glutathione-Sepharose beads. The beads were processed as described for (A), and the

protein eluates were analyzed by western blotting with an anti-RGS8 antibody (Pull-down, IB:RGS8). The amounts of GST fusion proteins loaded were verified by reprobing with an anti-GST antibody (IB:GST). The results are representative of three independent experiments. (Input) Samples showing the total amounts of purified proteins used for the reactions.

**Fig. 2. RGS8 and Flag-MCH1R colocalize at the cell membrane.**

**Upper panels,** Double-immunofluorescence staining of Flag-MCH1R and RGS8 in transfected HEK293T cells. HEK293T cells were transiently transfected with plasmid cDNAs encoding RGS8 (0.8  $\mu$ g) or Flag-MCH1R (0.2  $\mu$ g) plus RGS8 (0.8  $\mu$ g). At 24 h after transfection, the cells were incubated with or without 1  $\mu$ M MCH for 1 min. The cells were fixed, immunostained with an anti-Flag M2 and an anti-RGS8 antibodies and visualized using an FV1000 confocal microscope and imaging system. Green fluorescence at 488 nm (Flag tag), red fluorescence at 546 nm (RGS8) and merged images of the fluorescence are depicted. Yellow in the merged images indicates overlapping of the localizations. Untransfected cells incubated with the anti-RGS8 antibody showed no staining. Each image is representative of at least 42 cells examined under each condition derived from three independent experiments. Bars, 10  $\mu$ m. **Lower panels,** Expression of RGS8 protein in HEK293T cells used for the double-immunofluorescence staining shown in the upper panels. Total protein extracts (left) or membrane fractions (right) were resolved by SDS-PAGE using a 15% gel and transferred to a PVDF membrane. After immunoblotting with an anti-RGS8 antibody (IB:RGS8), the membrane was stripped and sequentially reprobed with an anti-actin antibody (IB:actin) and anti-G $\alpha$ q antibody (IB:G $\alpha$ q).

**Fig. 3. RGS8 inhibits MCH1R-mediated calcium signaling in a dose-dependent manner.**

**Upper panel,** Dose-response relationships of MCH-stimulated calcium mobilization in HEK293T cells expressing Flag-MCH1R in combination with RGS8. HEK293T cells on 6-well plates were transfected with Flag-MCH1R (0.2  $\mu$ g) and the indicated amounts of RGS8 or vector plasmid

pcDNA3.1 alone (1.0 µg; Mock). Vector plasmid was added to keep the total amount of DNA constant (1 µg). At 24 h after transfection, the cells were reseeded on 96-well plates. After loading with a non-wash calcium dye, MCH was added for 80 s and alterations in the calcium mobilization were monitored using a Flexstation II imaging plate reader. Data represent the means ± SEM of triplicate determinations. An additional experiment gave similar results. **Lower panel**, Western blot analysis of RGS8 expressed in the cells used for the functional assays shown in the upper panel. Total protein extracts from cell lysates were resolved by SDS-PAGE using a 15% gel and transferred to a PVDF membrane. After immunoblotting with an anti-RGS8 antibody (IB:RGS8), the membrane was stripped and reprobed with an anti-actin antibody (IB:actin).

**Fig. 4. The N-terminal domain mediates the interaction of RGS8 with MCH1R.**

**A**, N-terminal sequences of RGS8 and RGS8S. The rat RGS8S cDNA encodes 7 unique N-terminal amino acids instead of the typical amino acids 1-9 of rat RGS8, while the rest of RGS8S is the same as RGS8. **B, (Upper)** Dose-response relationships of MCH-stimulated calcium mobilization in HEK293T cells expressing Flag-MCH1R in combination with RGS8, RGS8S and RGS8 mutants. HEK293T cells on 6-well plates were transfected with Flag-MCH1R with or without the indicated amounts of RGS8, RGS8S, RGS8 mutants or vector plasmid pcDNA3.1 alone (Mock). Vector plasmid was added to keep total amount of DNA constant (1 µg). The ΔN9 deletion mutant lacks the first 9 amino acids of RGS8, but retains the intact RGS domain and C-terminus of the protein. In the L153F mutant, Leu153, a highly conserved residue in the RGS domain, is replaced with Phe, and this mutant is deficient in Gα binding. After loading with a non-wash calcium dye, MCH was added for 80 s and alterations in the calcium mobilization were monitored using a Flexstation imaging plate reader. Data represent the means ± SEM of triplicate determinations. **(Lower)** Western blots of RGS8, RGS8S, ΔN9 and L153F expressed in the cells used for the functional assays shown in the upper panel. Total protein extracts from cell lysates were resolved by SDS-PAGE using a 15% gel and transferred to PVDF membranes. After blotting with an anti-RGS8 antibody (IB:RGS8), the membranes were

stripped and reprobed with an anti-actin antibody (IB:actin). **C**, Binding profiles of His-RGS8 and His-ΔN9 to the MCH1R-i3 loop. 6xHis-RGS8 and His-ΔN9 were expressed in *E. coli* and purified by nickel-nitrilotriacetic acid affinity chromatography. Purified His-RGS8 and His-ΔN9 (1 μg each) were incubated with 2 μg of GST-MCH1R-i3 or GST alone and bound to glutathione-Sepharose beads. The beads were processed as described in the Experimental procedures, and the protein eluates were analyzed by western blotting with an anti-RGS8 antibody (Pull-down, IB:RGS8). The amounts of GST fusion proteins loaded were verified by reprobing with an anti-GST antibody (IB:GST). The results are representative of three independent experiments. (Input) Samples showing the total amounts of purified proteins used for the reactions.

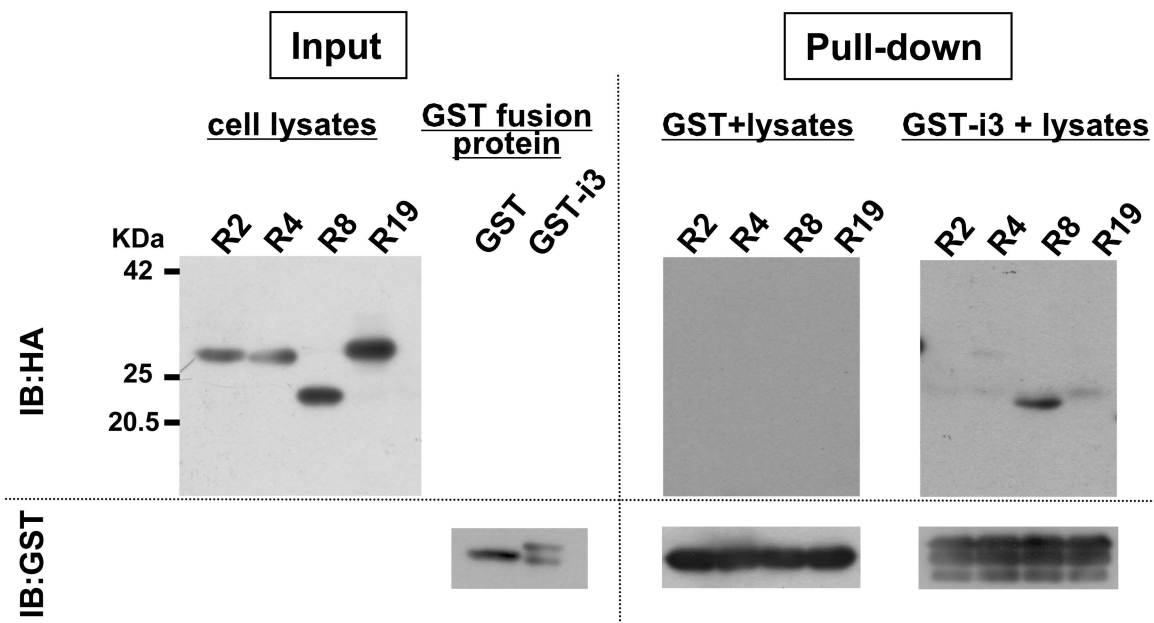
**Fig. 5. The distal end of the i3 loop in MCH1R is influential for the interaction with RGS8.**

**A**, Protein expression of Flag-MCH1R, mutant receptors and RGS8 in HEK293T cells. R253Q/R256Q or K252Q/R253Q/R256Q mutant receptors (0.2 μg) were transiently transfected into HEK293T cells seeded in 6-well plates with either pcDNA3.1 vector or RGS8 (0.8 μg). **(left)** Total protein extracts from cell lysates were separated by SDS-PAGE using a 12.5% gel and analyzed by immunoblotting with an anti-Flag M2 antibody (IB:M2). Several major immunoreactive bands (44, 45 and 60 kDa) are present in cells transfected with Flag-MCH1R. The same bands are also present in cells transfected with mutant receptors alone (R253Q/R256Q and K252Q/R253Q/R256Q) or in combination with RGS8. After blotting with the anti-Flag M2 antibody, the membrane was stripped and reprobed with an anti-actin antibody (IB:actin). **(right)** Total protein extracts from the cell lysates were resolved by SDS-PAGE using a 15% gel and immunoblotted with an RGS8 antibody (IB:RGS8). After immunoblotting with the anti-RGS8 antibody, the membrane was stripped and reprobed with an anti-actin antibody (IB:actin). **B**, Dose-response relationships of MCH-stimulated calcium mobilization in HEK293T cells expressing mutant receptors with RGS8 or without RGS8. Cells transfected with R253Q/R256Q or K252Q/R253Q/R256Q mutant receptors (0.2 μg) with either pcDNA3.1 vector or RGS8 (0.8 μg) were reseeded on 96-well plates. After loading with a non-wash

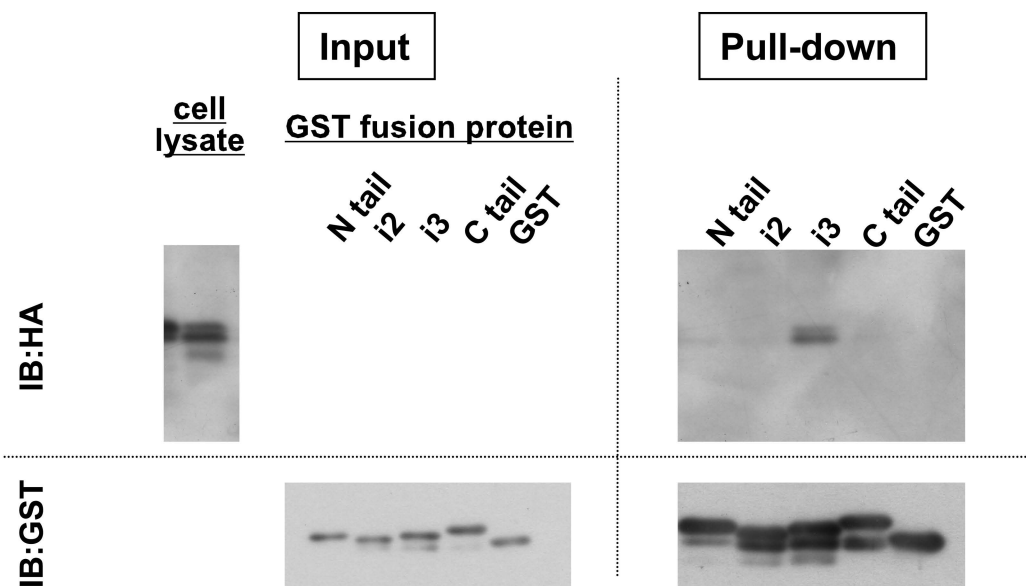
calcium dye, MCH was added for 80 s and alterations in the calcium mobilization were monitored using a Flexstation II imaging plate reader. Data represent the means  $\pm$  SEM of two separate experiments performed in duplicate. **C**, Binding profiles of His-RGS8 to the MCH1R-i3 and R253Q/R256Q-i3 loops. 6xHis-RGS8 was expressed in *E. coli* and purified by nickel-nitrilotriacetic acid affinity chromatography. Purified His-RGS8 (1  $\mu$ g) was incubated with 2  $\mu$ g of GST-MCH1R-i3 (GST-i3), GST-i3-R253Q/R256Q or GST alone, and bound to glutathione-Sepharose beads. The beads were processed as described in the Experimental procedures, and the protein eluates were analyzed by western blotting with an anti-RGS8 antibody (Pull-down, IB:RGS8). The amounts of GST fusion proteins loaded were verified by reprobing with an anti-GST antibody (IB:GST). The results are representative of three independent experiments. (Input) Samples showing the total amounts of purified proteins used for the reaction

# Fig.1

## A



## B



## C

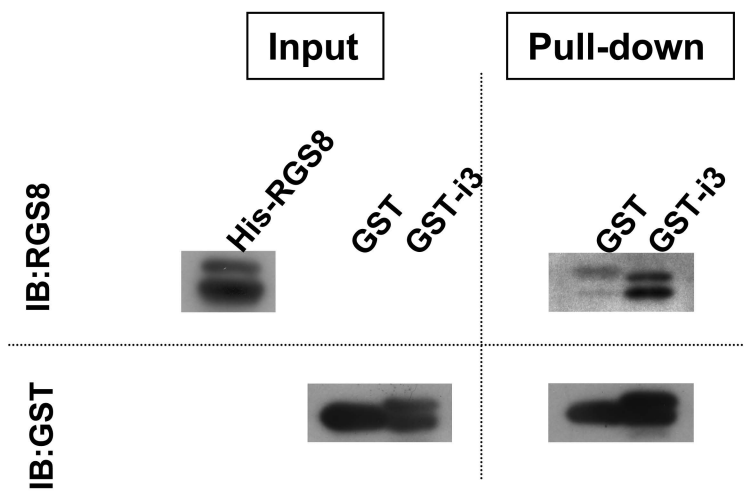


**Fig.2**

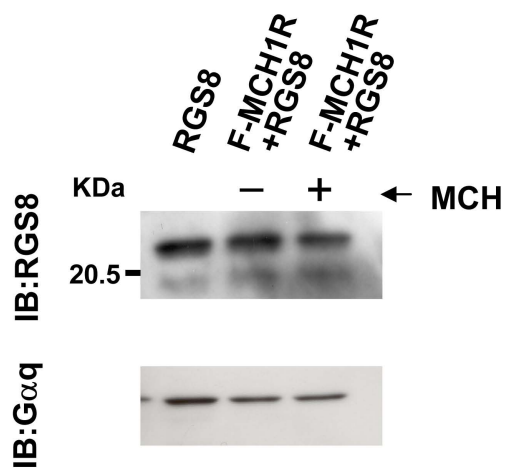
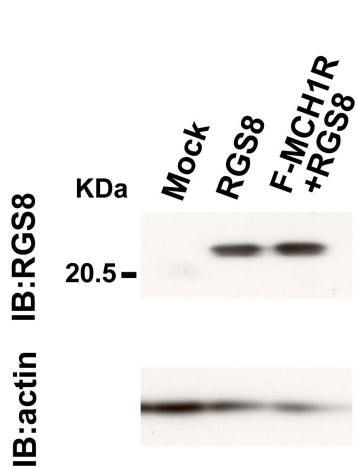
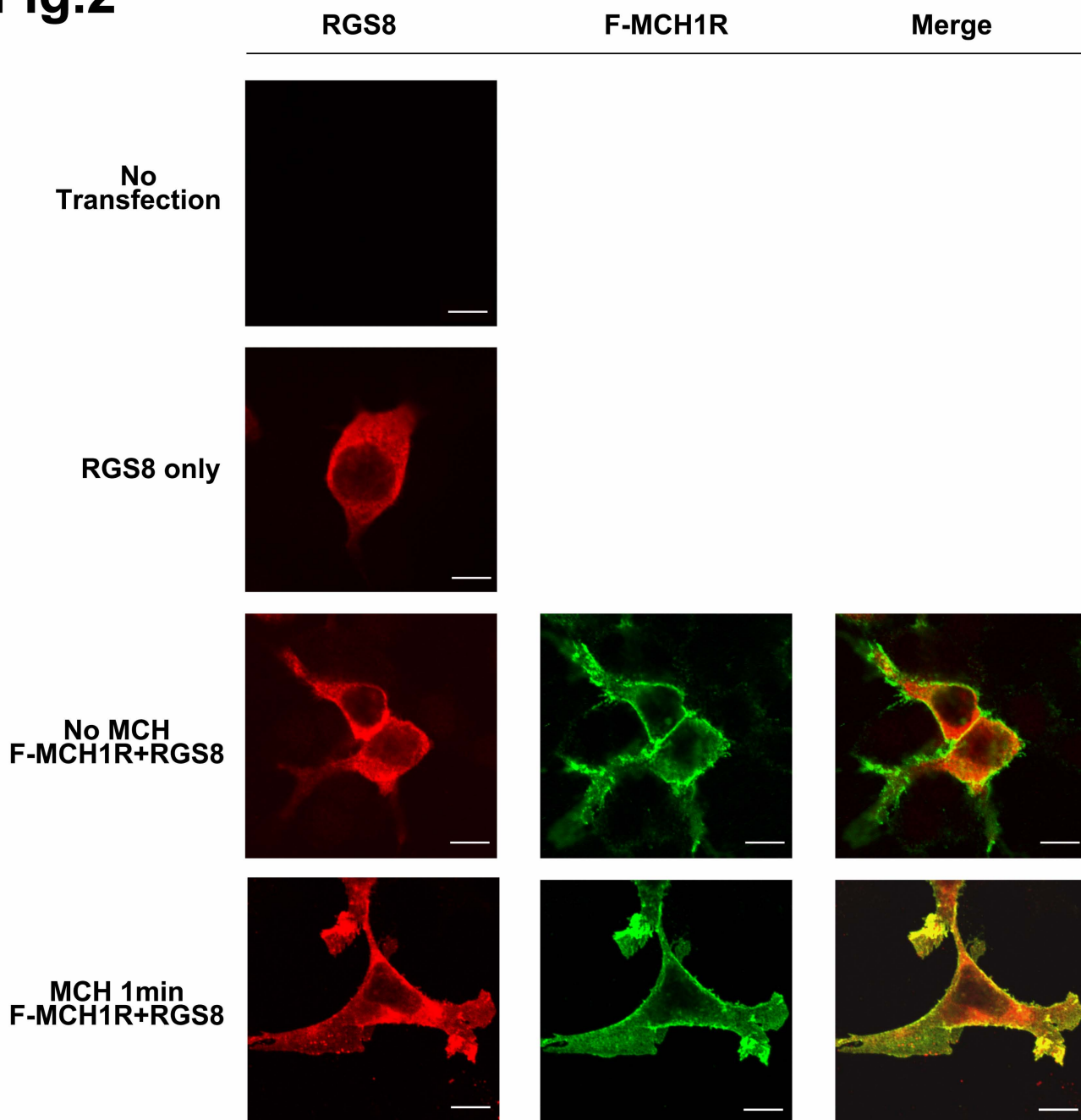


**Fig.3**

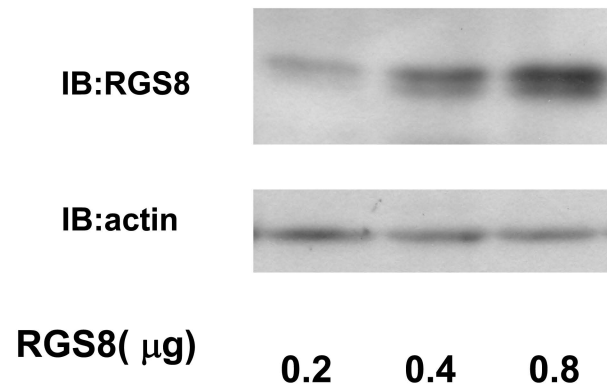
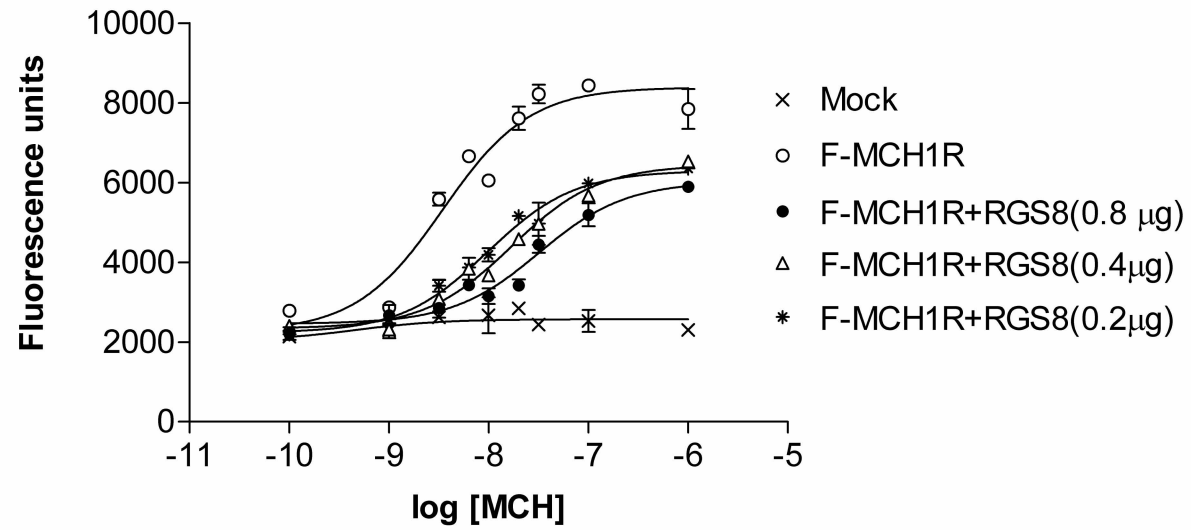
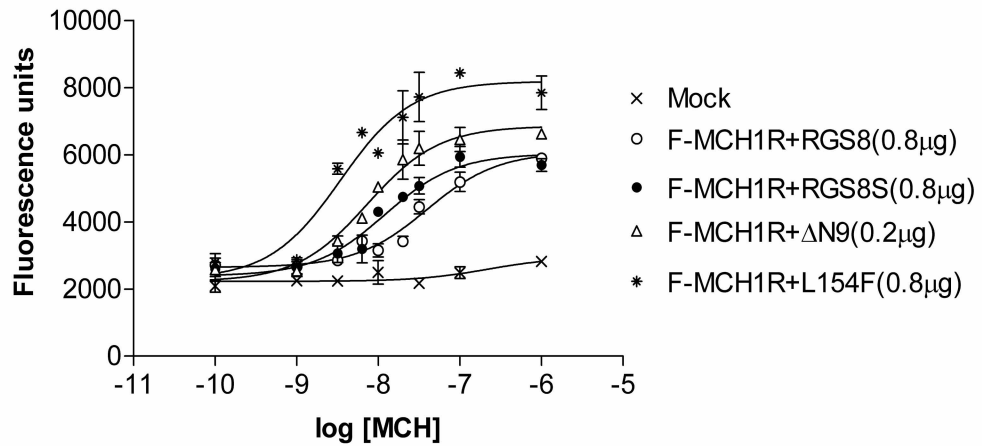


# Fig.4

**A**

	1	2	3	4	5	6	7	8	9	10	11	12
<b>RGS8</b>	M	A	A	L	L	M	P	R	R	N	K	G
<b>RGS8S</b>			M	R	T	G	Q	Q	Q	N	K	G

**B**



IB:RGS8



IB:actin



**F-MCH1R**

+ + +  
RGS8 RGS8S L154F  
(0.8µg) (0.8µg) (0.8µg)

**F-MCH1R**

+ + + +  
RGS8 RGS8 ΔN9 ΔN9  
(0.2µg) (0.8µg) (0.2µg) (0.8µg)

**C**

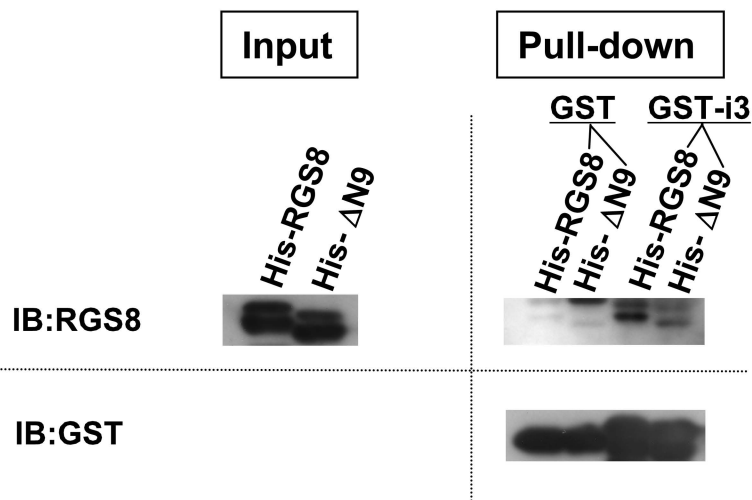
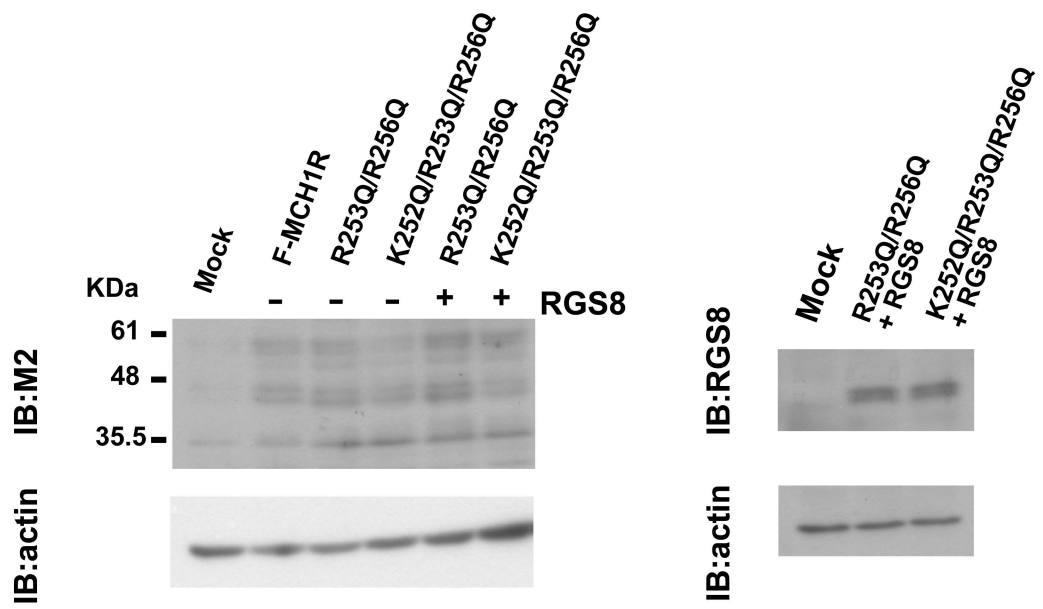
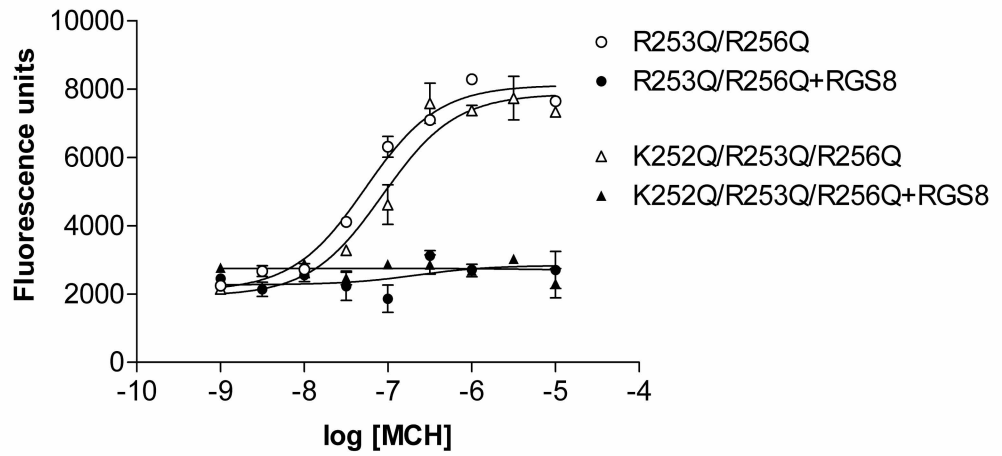


**Fig.5**

**A**



**B**



**C**

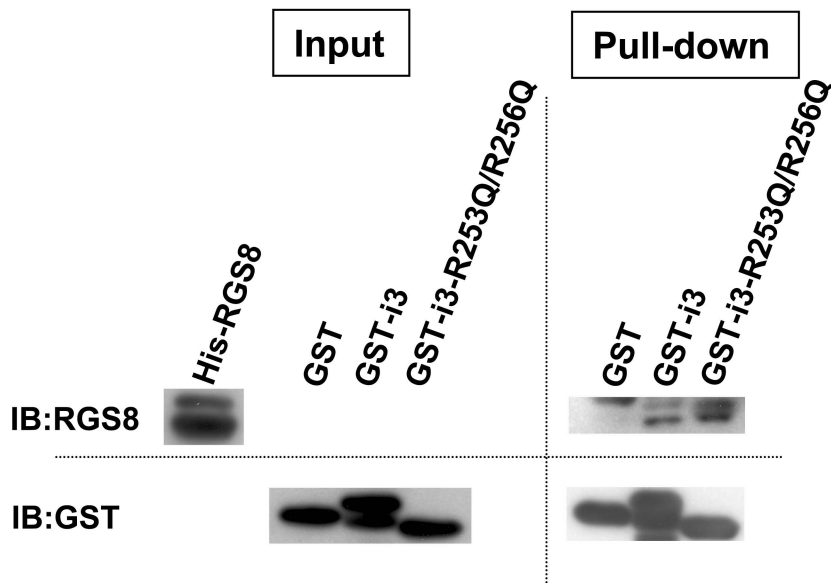


Table 1. MCH1R and M1 mAChR signaling with various combinations of RGS8 evaluated by calcium mobilization

Combination of MCH1R with RGS	EC50 value of ligand (nM) (fold)	Max Response (%)
F-MCH1R	1.3 ± 0.3 (1)	100
F-MCH1R + RGS8 (0.2µg)	9.1 ± 1.5 (7)	81.9 ± 3.9
F-MCH1R + RGS8 (0.4µg)	16.0 ± 4.7 (12.3)	83.4 ± 1.6
F-MCH1R + RGS8 (0.8µg)	24.7 ± 5.3 (19)	79.8 ± 3.4
F-MCH1R + RGS8S (0.8µg)	10.9 ± 1.6 (8.4)	82.6 ± 7.7
F-MCH1R + L153F (0.8µg)	1.5 ± 0.2 (1.2)	102.3 ± 2.5
F-MCH1R + ΔN9 (0.2µg)	10.2 ± 0.8 (7.8)	90.2 ± 6.9
M1 mAChR	13.3 ± 2.9 (1)	100
M1 mAChR + RGS8 (0.8µg)	206.6 ± 13.8 (15.5)	93.5 ± 5.4
M1 mAChR + RGS8S (0.8µg)	37.1 ± 5.4 (2.8)	115.0 ± 5.2
M1 mAChR + ΔN9 (0.2µg)	32.8 ± 5.9 (2.5)	105.0 ± 8.5

HEK293T cells on 6-well plates were transfected with Flag-MCH1R (0.2 µg) or M1 mAChR (0.2 µg) with or without RGS8, RGS8S or RGS8 mutants. Vector plasmid pcDNA3.1 was added to keep the total amount of DNA constant (1 µg). Transfected cells reseeded on 96-well plates were loaded with a non-wash calcium dye. The level of intracellular Ca<sup>2+</sup> ([Ca<sup>2+</sup>]<sub>i</sub>) induced by MCH or carbachol was detected using a Flexstation II imaging plate reader over an 80-s stimulation period. Data represent the means ± SEM of at least three independent experiments performed in duplicate.

Table 2. EC50 values of MCH for  $[Ca^{2+}]_i$  for various mutants of the MCH1R-i3 loop with RGS8

Receptor	No RGS8 (nM)	+ RGS8 (nM)	Ratio
F-MCH1R	1.5 ± 0.4	23.8 ± 4.2	16.0
R248Q	1.4 ± 0.3	22.6 ± 3.6	16.1
K252Q	1.3 ± 0.2	19.4 ± 3.1	14.9
R253Q	4.5 ± 1.1	72.6 ± 8.6	16.0
R256Q	5.0 ± 1.3	71.2 ± 5.2	14.2
R253Q/R256Q	42.2 ± 2.6	None	-
K252Q/R253Q/R256Q	80.3 ± 7.5	None	-

HEK293T cells on 6-well plates were transfected with 0.2 µg of Flag-MCH1R or mutant receptors and 0.8 µg of RGS8 or vector plasmid pcDNA3.1. Data represent the means ± SEM of at least three independent experiments performed in duplicate.